

# Natural selection drives recurrent formation of activating killer cell immunoglobulin-like receptor and Ly49 from inhibitory homologues

Laurent Abi-Rached and Peter Parham

Department of Structural Biology, and Department of Microbiology and Immunology, Stanford University School of Medicine, Stanford, CA 94305

**Expression of killer cell Ig-like receptors (KIRs) diversifies human natural killer cell populations and T cell subpopulations. Whereas the major histocompatibility complex class I binding functions of inhibitory KIR are known, specificities for the activating receptors have resisted analysis. To understand better activating KIR and their relationship to inhibitory KIR, we took the approach of reconstructing their natural history and that of Ly49, the analogous system in rodents. A general principle is that inhibitory receptors are ancestral, the activating receptors having evolved from them by mutation. This evolutionary process of functional switch occurs independently in different species to yield activating KIR and Ly49 genes with similar signaling domains. Selecting such convergent evolution were the signaling adaptors, which are older and more conserved than any KIR or Ly49. After functional shift, further activating receptors form through recombination and gene duplication. Activating receptors are short lived and evolved recurrently, showing they are subject to conflicting selections, consistent with activating KIR's association with resistance to infection, reproductive success, and susceptibility to autoimmunity. Our analysis suggests a two-stage model in which activating KIR or Ly49 are initially subject to positive selection that rapidly increases their frequency, followed by negative selection that decreases their frequency and leads eventually to loss.**

NK cells are effector lymphocytes of innate immunity that respond to infection (1, 2), malignancy (3), and allogeneic hematopoietic transplantation (4); they also facilitate placentation in reproduction (5). NK cell responses are determined by batteries of activating and inhibitory receptors (6). Ligands for several NK cell receptors are MHC class I and structurally related molecules. The NK cell receptors that recognize polymorphic MHC class I molecules are themselves encoded by diverse, polymorphic, and rapidly evolving gene families that contribute to the diversity and repertoire of NK cell populations and T cell subpopulations (7, 8). Further emphasizing the evolutionary plasticity and versatility of these NK cell receptors, the analogous functions are performed by structurally unrelated glycoproteins in different species, as exemplified by the killer cell Ig-like receptors (KIR) of primates and the Ly49 receptors of rodents (9).

In contrast to MHC polymorphism, KIR polymorphism can affect a receptor's signal-

ing function as well as its binding to ligands. Activating function is effected by a positively charged residue in the transmembrane region, whereas inhibitory function is conferred by inhibitory tyrosine-containing immunomotifs (ITIM) in the cytoplasmic tail. Of the 14 human KIR, seven are inhibitory, six are activating, and one has dual function. The balance between activating and inhibitory receptors at the NK cell surface is reflected in the population genetics: *KIR* haplotypes divide into two functionally distinct groups according to their complexity and the content of genes encoding activating KIR (10). Group A haplotypes have only one activating *KIR* gene (*KIR2DS4*), and it is frequently disabled (11, 12). The more complicated group B haplotypes can have up to five of the six genes encoding activating receptors (*KIR2DS1–5* and *KIR3DS1*) as well as additional genes encoding inhibitory receptors (*KIR2DL5A* and *KIR2DL5B*). Consequently, human genotypes vary widely in their content of activating *KIR*, as do the frequencies in human populations (13). These distributions point

## CORRESPONDENCE

Peter Parham:  
peropa@stanford.edu

Abbreviations used: CYT, cytoplasmic tail; ITIM, inhibitory tyrosine-containing immunomotif; KIR, killer cell Ig-like receptor; LTK, long-tailed KIR; MYA, million yr ago; NJ, neighbor joining; STK, short-tailed KIR; TM, transmembrane domain.

The online version of this article contains supplemental material.

Supplemental material can be found at:  
<http://doi.org/10.1084/jem.20042558>

to distinctive and balancing selection for haplotypes that are rich or poor in activating *KIR*.

Certain pairs of *KIR* have similar extracellular domains but differ in their signaling function. Inhibitory receptors

specific for HLA-C, *KIR2DL1* and *KIR2DL2/3*, pair with the activating receptors *KIR2DS1* and *KIR2DS2*, respectively. Likewise, the inhibitory receptor for HLA-B, *KIR3DL1*, is paired with the activating receptor *KIR3DS1*.

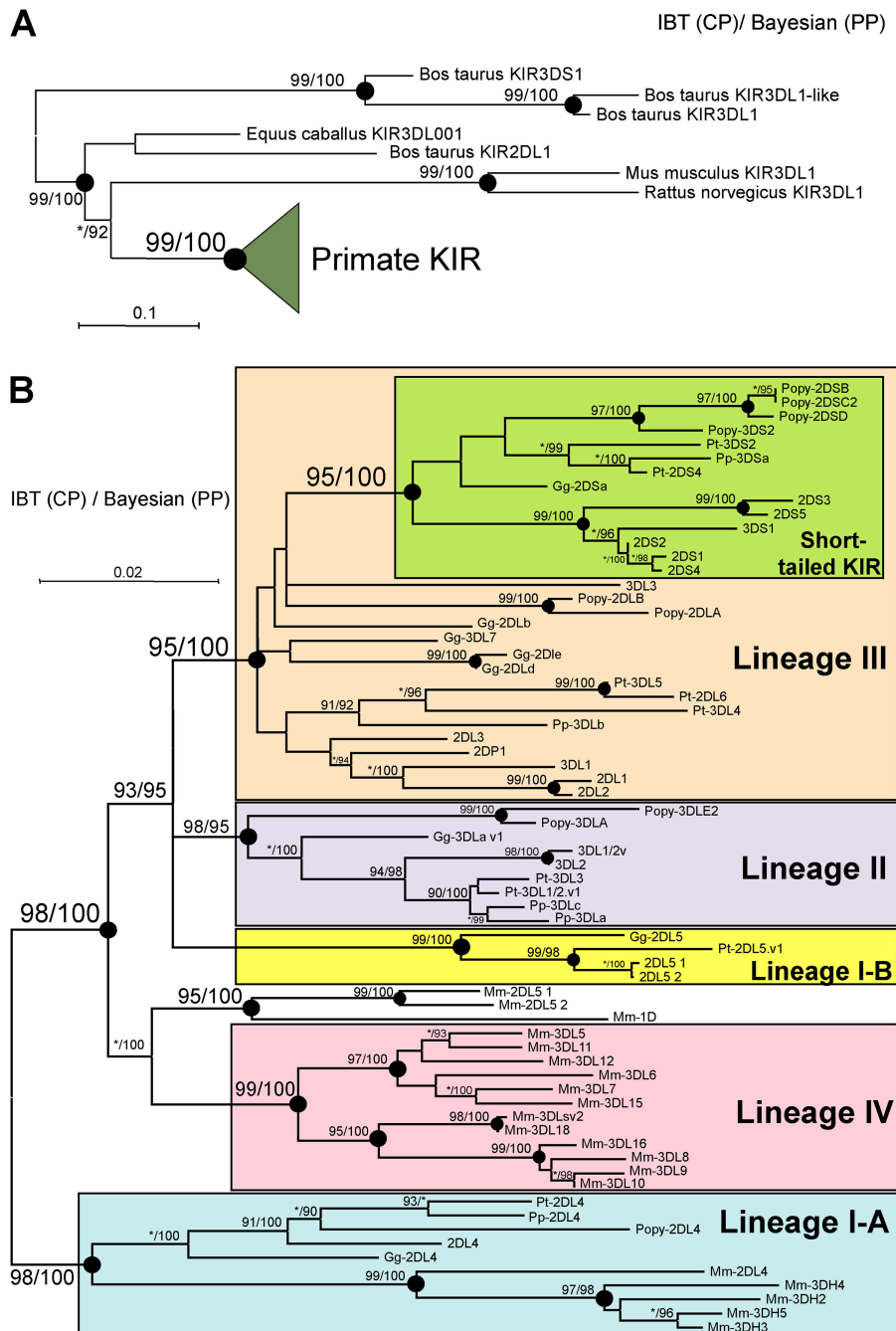


**Figure 1. The signaling domains of short-tailed hominoid *KIR* form a monophyletic group within lineage III *KIR*.** (A) Comparison of mammalian *KIR* signaling domains shows that primate sequences form a monophyletic group. To simplify the tree, the primate sequences were collapsed. (B) Among primate *KIR* the signaling domains of *short-tailed KIR* form a monophyletic group within lineage III (B). Neighbor joining (NJ) and Bayesian trees gave statistically similar topologies; the NJ topology is displayed (using a mid-

point rooting). Colored boxes denote the different *KIR* lineages. The statistical support for each node (expressed as a percentage) was given by the interior branch test confidence probability and the Bayesian posterior probability. Values are shown for nodes supported by  $\geq 90\%$  with one or both methods; asterisks indicate values  $< 90\%$ . Nodes marked by a filled circle were supported  $\geq 95\%$  by both methods. Gg, *Gorilla gorilla*; Mm, *Macaca mulatta*; Pt, *Pan troglodytes*; Pp, *Pan paniscus*; Popy, *Pongo pygmaeus*.

These relationships suggest how KIR signaling function might be switched, from activating to inhibitory, or vice versa, in the course of evolution (14). The ligand-binding specificities of the inhibitory receptors are well characterized, but similar studies of the activating receptors have met with limited success (15–18), although clinical correlations point to their interaction with HLA class I. For HIV infection, the combination of KIR3DS1 and certain HLA-B allotypes was correlated with slower progression to AIDS (19), and certain combinations of HLA-C with KIR2DS1 and KIR2DS2 correlate with autoimmune conditions (20–22). For infectious disease, the plausibility of such mechanisms is shown by the demonstration that the activating Ly49H variant provides specific resistance to cytomegalovirus infection in a mouse model (23).

Because of the evolutionary plasticity of MHC class I-specific NK cell receptors and the unprecedented species-specific differences they exhibit, it becomes important to un-

derstand the general principles by which these receptors—particularly the activating receptors—evolve. The overall similarity of activating and inhibitory KIR demonstrates their common origin but leaves unanswered questions as to which came first—activating or inhibitory KIR—and how the signaling function is switched. Using phylogenetic analysis and evolutionary reconstruction, we have examined the natural history of KIR and can now answer these questions with confidence. Similar analysis of rodent Ly49 demonstrated that these evolutionary processes are remarkably parallel.

## RESULTS

### Hominoid-specific evolution of activating KIR

Signaling functions are determined by basic residues of the transmembrane region (TM) that bind to activating adaptor molecules and of ITIMs in the cytoplasmic tail (CYT). In this paper, we define the combination of TM and CYT as the KIR signaling domain. Phylogenetic comparison of the

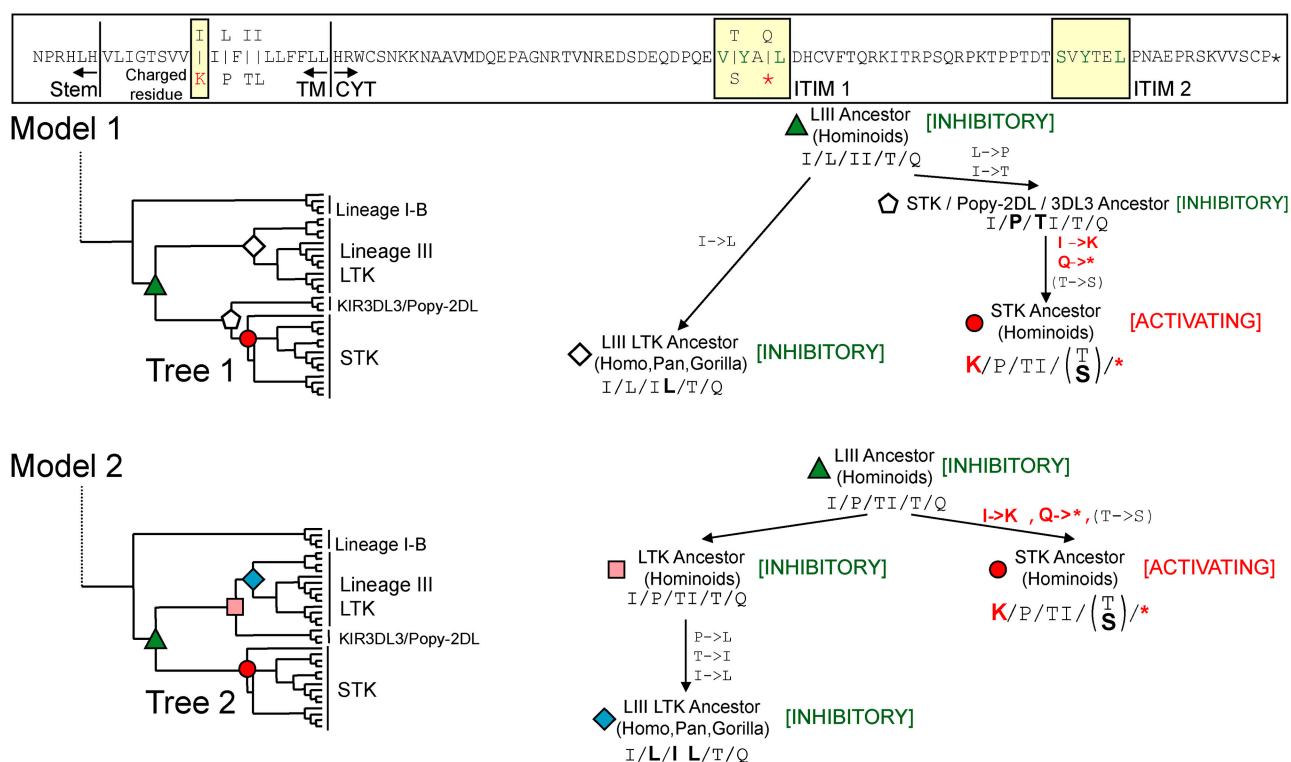


**Figure 2.** The STK ancestor evolved by functional switch of an inhibitory KIR. The signaling domain sequences of the STK, LTK, and lineage III ancestors were reconstructed. The upper panel shows the amino acid sequence. Residues common to the different predictions are indicated on the main line. For variable residues, the possibilities are indicated above and below the main line. The characteristic charged residue of activating KIR and the ITIM motifs of inhibitory KIR are boxed. Two models were used to perform the ancestral sequence reconstruction. The middle panel shows the first model. The tree topology corresponds to that obtained in the Bayesian analysis performed in Fig. 1; the relevant part of the tree is displayed. The bottom panel shows the second model. This topology represents a modification of the first topology in which the *KIR3DL3* and *Popy-*

*KIR2DLA/B* sequences are grouped with the lineage III *LTK* group. This modification is based on the result presented in Fig. 3 A. The trees on the left sides of the panels show the nodes corresponding to the reconstructed sequences. Empty symbols pertain to the marginal reconstruction method alone; filled symbols pertain to both the marginal reconstruction and Bayesian methods. Positions varying among the predicted sequences and corresponding to the variable positions in the upper panel are shown in the schemes on the right sides of the panels. The amino acid substitutions leading to the different groups are shown next to the arrows joining the groups. Residues that change along each branch are in boldface type. Parentheses show positions where marginal reconstruction and Bayesian methods gave different results.

sequences encoding the signaling domains of mammalian KIR shows that all primate KIR signaling domains form a monophyletic group (Fig. 1 A) and thus derive from one unique common ancestor. Within the primate KIR, the signaling domains of all the activating, short-tailed KIR (STK) of the hominoids (i.e., KIR2DS and KIR3DS) form a monophyletic group (Fig. 1 B). In contrast, the signaling domains of the long-tailed KIR (LTK; i.e., KIR2DL and KIR3DL) segregate into several groups, corresponding chiefly to the lineages defined from cDNA sequences (24). In the same phylogenetic tree, the STK all group with the LTK of lineage III, which includes the HLA-C-specific KIR (Fig. 1 B). In summary, the signaling domains of all modern hominoid KIR2DS and KIR3DS derive from a unique hominoid ancestor that was a lineage III KIR.

### Activating KIR evolved from inhibitory KIR

Trees constructed for the primate signaling domain comprise two deep clades, one containing *KIR2DL4* and related KIR (lineage I-A) and the other that divides into related groups of KIR corresponding to the lineage I-B, II, III, IV, and rhesus monkey *KIR2DL5* and *KIR1D* (Fig. 1 B). Whereas all these subclades contain inhibitory LTK, only lineage III also contains activating STK. That the STK are deeply nested within the lineage III KIR indicates that the ancestral lineage III KIR was a LTK rather than a STK. The ancestral STK would then have evolved from a lineage III LTK with accompanying functional switch. To assess the validity of this model, we reconstructed the sequences for the signaling domain of the last common ancestor of the STK, the lineage III LTK, and of all lineage III KIR (Fig. 2). Because the relative positions of three sequences (*KIR3DL3* and *Popy-KIR2DLA/B*) within the lineage III were uncertain, two alternative trees were used to reconstruct the ancestral sequences. For each alternative tree, the results of two

independent methods of analysis indicated that the last common ancestor of the lineage III KIR was an inhibitory LTK (Fig. 2).

These reconstructions of ancestral sequence were also used to predict the amino acid substitutions that formed the ancestral STK. Two amino acids were identically predicted by the two analytical methods (Fig. 2). These substitutions are precisely those that switch the receptor's function from inhibition to activation. Activating function was gained by introduction of a positive charge (K) into the TM, through which STK interact with the DAP12 adaptor (25, 26). Inhibitory function was lost by introduction of a stop codon within the membrane proximal ITIM motif of the CYT. Because both changes occurred in the same evolutionary branch, it is not possible to determine which occurred first. That the evolution of the ancestral STK involved only substitutions that directly affected signaling function is indicative of selection.

To assess the impact of natural selection on KIR signaling domains, we estimated their mean number of synonymous substitutions per synonymous nucleotide site ( $d_s$ ) and number of nonsynonymous substitutions per nonsynonymous nucleotide site ( $d_N$ ) (Table I). Although seven of the nine groups analyzed show an excess of synonymous substitutions ( $d_N/d_s < 1$ ), for six groups it did not reach statistical significance. Such evidence for weak purifying selection can be attributed to the small size of the signaling domain (63 aa) and the relatively few residues in the TM and CYT domains that are functionally critical. Many other positions, however, are likely to tolerate a range of substitutions, for example hydrophobic substitutions in the TM. The KIR group showing statistically significant purifying selection ( $P < 0.05$ ) was the STK. Because the analysis was performed on present-day STK sequences, it did not include the functionally important substitutions that produced the functional shift; rather, it in-

**Table I.** Mean number of synonymous substitutions per synonymous site ( $d_s$ ) and nonsynonymous substitutions per nonsynonymous site ( $d_N$ ) substitutions within the different KIR lineages/groups for the TM and CYT (partial) domains

	$d_N$ (*100) <sup>a</sup>	Standard error (*100) <sup>a</sup>	$d_s$ (*100) <sup>a</sup>	Standard error (*100) <sup>a</sup>	$d_N/d_s$	Z-value	P ( $d_N = d_s$ )
STK	3.62	1.02	8.95	2.34	0.40	-2.07	<0.05
Lineage IA	8.30	1.66	4.96	2.08	1.67	1.20	NS
Lineage IB	0.85	0.59	2.93	1.64	0.29	-1.18	NS
Lineage II	3.51	1.02	5.02	1.79	0.70	-0.72	NS
Lineage III LTK (Homo, Pan, Gorilla)	4.79	0.97	5.48	1.73	0.87	-0.34	NS
<i>Popy-KIR2DL (A/B)</i> <i>KIR3DL3</i>	4.35	1.32	5.23	2.50	0.83	-0.30	NS
Lineage III LTK (Hominoids)	5.96	1.05	6.44	1.63	0.93	-0.24	NS
Lineage IV	3.32	1.04	3.30	1.28	1.00	0.01	NS
<i>Mm-KIR2DL5 (0.1/0.2)</i> <i>Mm-KIR1D</i>	6.55	1.64	9.70	3.33	0.68	-0.94	NS

<sup>a</sup>Values were multiplied by 100 to simplify the presentation.

**Table II.** Divergence times for the emergence of the activating KIR and Ly49

Group	Node	Limit	Mean (MYA)	95% confidence interval (MYA)
STK, model 1	Root <i>STK</i>	lower	13.2 ± 1.8	10.5–17.5
	Root lineage III	upper	18.2 ± 2.3	14.1–23.2
STK, model 2	Root <i>STK</i>	lower	13.6 ± 1.9	10.6–18.0
	Root lineage III	upper	18.0 ± 2.4	13.7–23.1
<i>Mm-KIR3DH</i>	<i>Mm-KIR3DH</i> / <i>Mm-KIR2DL4</i>		10.3 ± 2.7	5.9–16.2
Activating <i>Ly49</i>	Root activating <i>Ly49</i>	lower	18.5 ± 2.4	14.3–23.2
	Root rodent <i>Ly49</i>	upper	31.1 ± 4.2	24.1–40.4
Rat <i>Ly49s3</i>	<i>Ly49s3/Rno (1)</i>	lower	3.5 ± 2.1	0.4–8.7
	<i>Ly49s3/Rno (6)</i>	upper	15.7 ± 3.1	9.9–22.1

volved only substitutions that occurred after the shift. The result shows that, in the subsequent evolution and expansion of the STK family, purifying selection has preserved the structure of the signaling domain and its activating function.

To date, STK have been characterized only in hominoids. To assess the likelihood that other primate species possess STK, we estimated a time range for occurrence of the functional switch that gave rise to the STK ancestor (Table II). This analysis was performed for the two models shown in Fig. 2. For both models, the lower limit of the range, which corresponds to the last common ancestor of all STK, was estimated at ~13.5 million years ago (MYA). The upper limit of the range, which corresponds to the last common ancestor of all lineage III KIR, was estimated at ~18 MYA. The range of 13.5 to 18 MYA indicates that STK may exist in hylobatids (gibbons and siamangs), because their divergence from other hominoids is estimated to have occurred 16.5–18.5 MYA (27). On the other hand, STK are unlikely to be found in Old World monkeys. Although estimates of the Old World monkey–hominoid divergence time vary, most evidence points toward a minimum of 23 MYA (28), corresponding to the upper limit of the 95% confidence interval for the upper range of the STK emergence (Table II).

#### Expansion of the STK occurred mainly by recombination

After the formation of the first *STK* gene in a hominoid ancestor, a family of hominoid *STK* genes was formed by expansion, as exemplified by the presence of several *STK* genes in modern humans, orangutans, and common chimpanzees. Although duplication of a complete gene is a necessary mechanism for the expansion of gene families, we previously showed that recombination between genes has been the main mechanism generating new *KIR* (24). To investigate the mechanisms that diversified and expanded the *STK*, we performed a domain-by-domain phylogenetic analysis. Trees constructed from the signaling domain of the lineage III *KIR* revealed four subclades within the *STK* clade. These subclades divide along species-specific lines: human, gorilla, orang-

utan, and the two chimpanzees (Fig. 3 A). Within each species or pair of species, the modern *STK* derive from a single common ancestor. The tight clustering of the *STK* in the signaling-domain tree does not extend to trees constructed for the extracellular domains D2 (Fig. 3 B), D1 (Fig. 3 C), and D0 (Fig. 3 D). Here the *STK* are distributed among various branches of the lineage III *KIR* and are also found in other *KIR* lineages (Fig. 3). From domain to domain, the phylogenetic relationships between the *STK* differ, evidence for their diversification by recombination.

Three *STK*—bonobo *Pp-KIR3DSA*, orangutan *Popy-KIR3DS2*, and human *KIR3DS1*—have extracellular domains that cluster with lineage II *KIR*. Each of these *KIR* was formed by an interlineage recombination in which the Ig domains of a lineage II *KIR* combined with the signaling domain of an activating lineage III *KIR2D*. That *Pp-KIR3DSA*, *Popy-KIR3DS2*, and *KIR3DS1* are not nearest neighbors in the signaling domain tree (Fig. 3 A) argues against their being orthologous *KIR* and for their formation by independent recombination events in bonobo, orangutan, and human evolution. That independent acquisition of an activating *KIR3D* occurred in each of these species provides a striking example of parallel (convergent) evolution. A further product of interlineage recombination is *Pt-KIR3DS2*, for which the D0 domain clusters with lineage V *KIR* (Fig. 3 D).

For the remaining 10 *STK*, all the domains are of lineage III. Reconstruction of their histories is hindered by lack of resolution in the D2 domain tree (Fig. 3 B) and, to lesser extent, in the D1 domain tree (Fig. 3 C). The D0 domain tree (Fig. 3 D) is well resolved and shows that five *STK* (*Gg-KIR2DSa*, *KIR2DS3*, *KIR2DS5*, *Pt-KIR2DS4*, and *KIR2DS4*) form a cluster resembling that for the signaling domain (Fig. 3 A). *Gg-KIR2DSa*, *Pt-KIR2DS4*, and *KIR2DS4* may represent orthologues, whereas *KIR2DS3* and *KIR2DS5* are probably products of gene duplication. In contrast, *KIR2DS1* and *KIR2DS2* are recombinants, as seen from their distinctive positions in the trees for the D0 domain and the signaling domain. In summary, of the 14 *STK*,

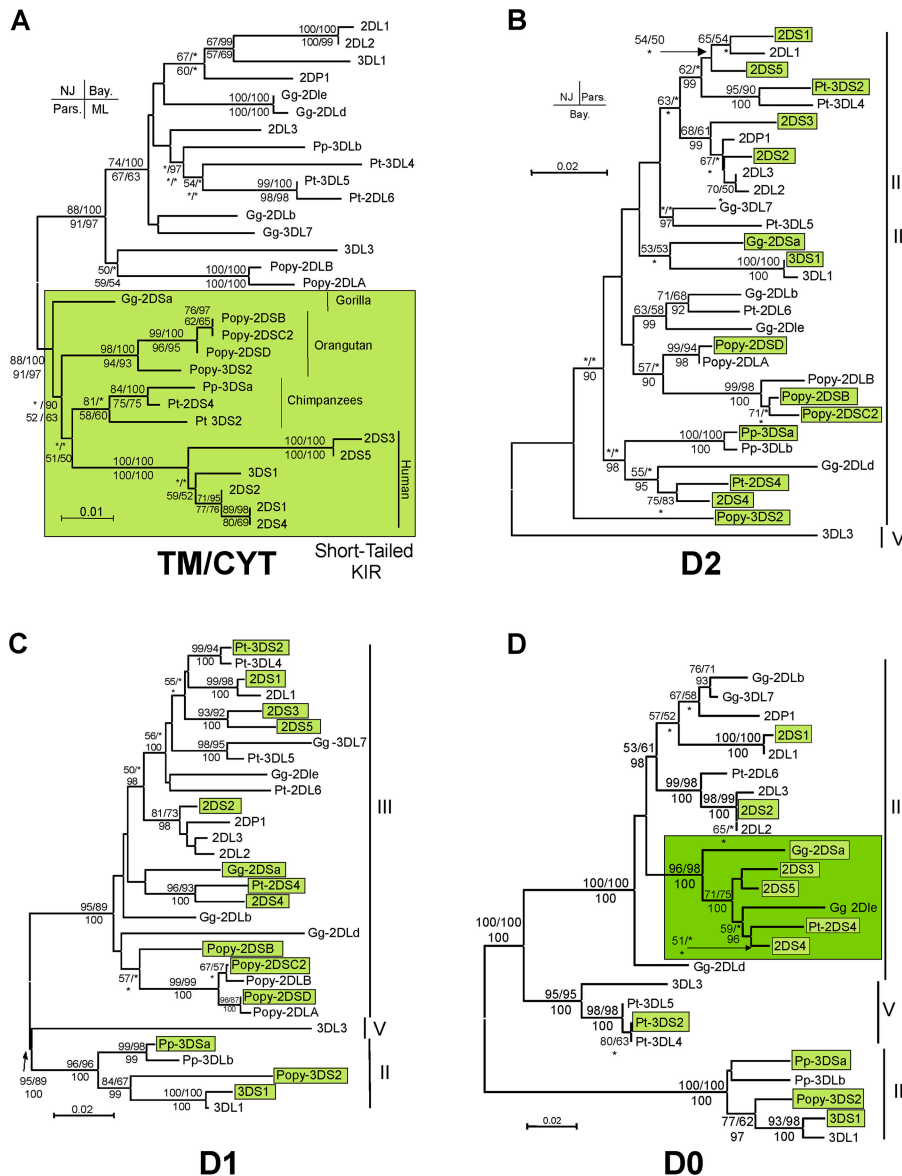


**Figure 3. Expansion of the *STK* was driven mainly by recombination.** Phylogenetic trees were constructed for nucleotide sequences corresponding to each domain of the lineage III *KIR* defined in Fig. 1: (A) TM/CYT-signaling domain; (B) D2 domain; (C) D1 domain; (D) D0 domain. The *KIR* lineages are labeled on the right side of each panel. Shaded boxes denote the *STK* sequences. NJ, parsimony (Pars), and Bayesian (Bay) methods gave trees with statistically similar topology; the NJ trees are shown (using a midpoint rooting). The support for each node (expressed as a percentage) was given by the NJ and parsimony bootstrap proportion and by the Bayesian posterior probability. Values are shown for nodes supported by  $\geq 50\%$  for

the bootstrap proportion analyses and by  $\geq 90\%$  for the posterior probability analysis. Asterisks indicate values below these cutoffs. For the signaling domain (A) a fourth test, a maximum-likelihood bootstrap analysis, was performed; the bootstrap proportion was estimated for each node and indicated where  $\geq 50\%$ . At nodes the support for the four methods (NJ, Bayesian, parsimony, and maximum likelihood) are organized as shown in the upper left. Species abbreviations are as in Fig. 1. All the analyses were performed with a complete deletion dataset (supplemental Material and methods). (D) A group of sequences potentially corresponding to the *STK* group is boxed.

six are clearly products of recombination, four are possibly orthologues, and two are the products of gene duplication. The remaining two *STK* are the orangutan *KIR2D*, for which the genomic sequences corresponding to the D0 domains are not known; they could be products of either gene duplication or recombination.

**Distinctive signaling domain in activating monkey *KIR***

In hominoids, *KIR2DL4* seems to be unique because it is a LTK with activating function (29–31) and because of its ubiquitous expression by NK cells. *KIR2DL4* is also the only *KIR* that is shared by hominoids and Old World monkeys, represented in our study by the rhesus macaque. Be-

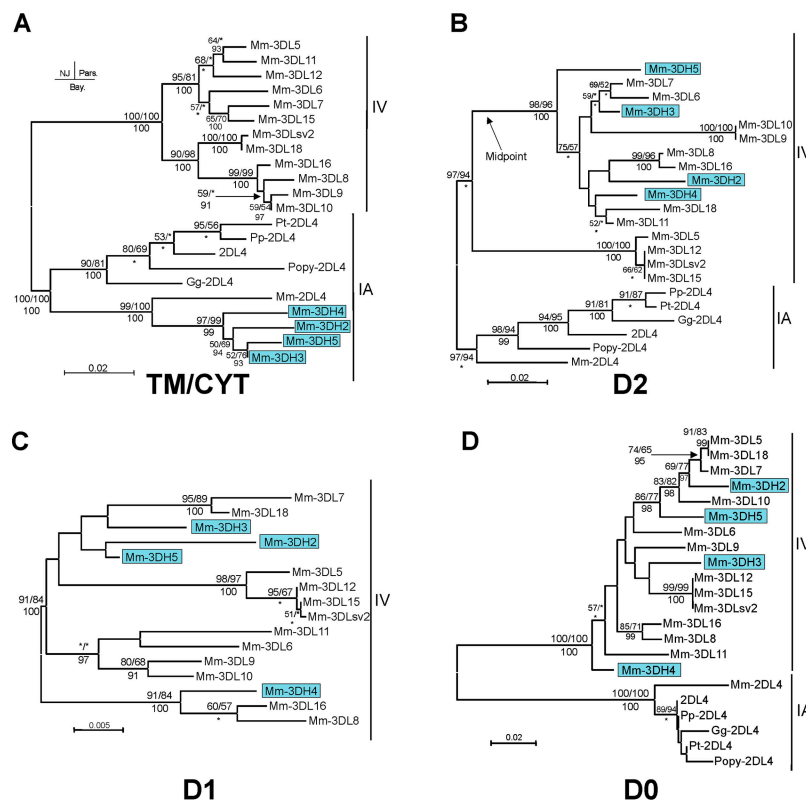


**Figure 4. Rhesus monkey activating 3Ig KIR use a modified KIR2DL4 signaling domain.** Phylogenetic trees were constructed for nucleotide sequences corresponding to each domain of the lineage I–A and IV KIR defined in Fig. 1: (A) TM/CYT signaling domain; (B) D2 domain (the tree was rerooted because the midpoint rooting was influenced by the long

branch of the group containing *Mm-KIR3DL9* and *Mm-KIR3DL10*); (C) D1 domain; (D) D0 domain. Tree construction, evaluation, and statistical tests were as described in the legend of Fig. 3; representative NJ trees are shown. Species abbreviations are as in Fig. 1.

sides the *KIR2DL4* orthologue, the rhesus macaque has several *Mm-KIR3DH* (32, 33) for which the signaling domain resembles that of *KIR2DL4* (Fig. 4 A). This similarity does not extend to the Ig-like domains (Fig. 4, B–D) where the four *Mm-KIR3DH* cluster in lineage IV with the other *Mm-KIR3D*. The *Mm-KIR3DH* are activating receptors formed by recombining the signaling domain of *Mm-KIR2DL4* with the extracellular domains of *Mm-KIR3D*. Unlike *KIR2DL4*, they do not express exon 8 (32, 33), which causes a frame shift that eliminates the two ITIMs of the *Mm-KIR2DL4* tail and leaves *Mm-KIR3DH* with only activating potential. The similarity of the signaling domain in the four *Mm-KIR3DH* shows that recombination between *Mm-KIR2DL4* and *Mm-KIR3DL* occurred only once. We estimate this event took place  $\sim 10.5$  MYA (Table II), a time close to the divergence of Cercopitheciini (guenons, green monkeys, and patas monkeys) from Papionini (macaques and Papionina),  $\sim 8$ – $9.5$  MYA (27), probably after the separation of colobines (leaf-eating monkeys) and cercopitheciines (cheek-pouched monkeys),  $\sim 13$ – $14$  MYA (27), and before the macaques diverged from the Papionina (baboons, mangabays, and mandrills),  $\sim 7$ – $8$  MYA (27). We predict, therefore, that *KIR3DH* genes are present in all Papionini and

possibly in all living cercopitheciines but not in colobines. The Ig domain sequences of *Mm-KIR3DH*, particularly D0 (Fig. 4 D), are not monophyletic, suggesting the existence of more than one *Mm-KIR3DH* locus. Because the *Mm-KIR3DH* sequences do not cluster tightly in the Ig domain trees, the different loci probably evolved by recombination rather than gene duplication.

#### Activating KIR coopted more ancient signaling pathways

Parallel evolution formed activating NK receptors from inhibitory ones in hominoids and Old World monkeys. For hominoid STK, DAP12 is the signaling adaptor (25, 26), whereas for rhesus monkey KIR3DH it is probably FCER1G, which is also the signaling adaptor for KIR2DL4 (34). To determine whether the adaptor molecules evolved before, after, or at the same time as the activating KIR, we performed phylogenetic analyses on sequences from various species that were reported to resemble the signaling adaptors of human and murine immune receptors. This analysis revealed *DAP12*, *FCER1G*, and related *DAP10* and *CD3Z* are present and well conserved in several orders of mammals, as well as in amphibians and bony fishes (Fig. 5). These data strongly support a scheme in which *DAP12* and *FCER1G*

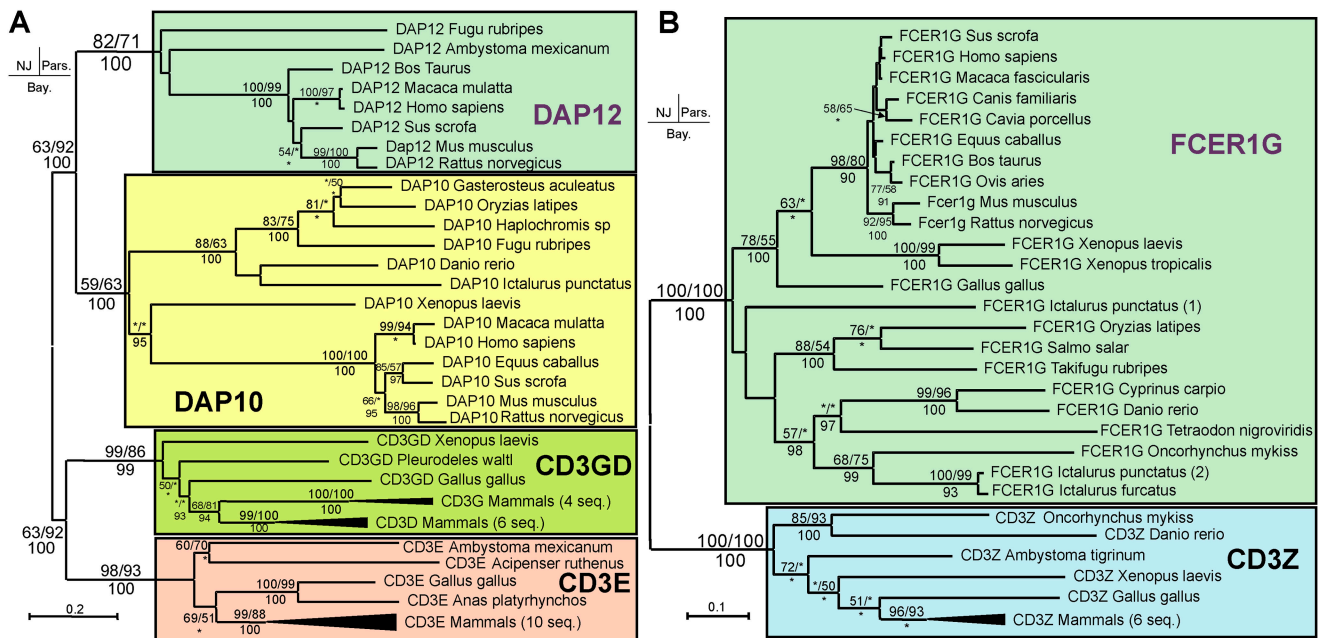


**Figure 5. Signaling adaptor molecules DAP12 and FCER1G existed long before the emergence of activating primate KIR and rodent Ly49 receptors.** Phylogenetic trees (A) of the *DAP12* family and (B) of the *FCER1G* family. Tree construction, evaluation, and statistical tests were as

in Fig. 3; representative NJ trees are shown. For simplification, some groups of sequences were collapsed; the number of the sequences in such groups is indicated.

emerged before separation of mammals and bony fishes, more than 400 MYA. Consequently, when activating KIR were formed in primates,  $\sim 13.5$ – $18$  MYA for the STK and  $\sim 10.5$  MYA for the rhesus monkey KIR3DH (Table II), they were able to coopt a preexisting signaling pathway. The implication is that the constraints imposed by the existing signaling pathways guided the evolution of the activating KIR by selecting for variants that could coopt such pathways.

#### Parallel evolution of activating rodent Ly49 and primate KIR

Although rodent genomes contain *KIR* genes, their properties and functions seem to be dissimilar to the hominoid *KIR* gene family (35). In mice and rats, the functional equivalent of KIR is Ly49, a structurally divergent family of lectinlike glycoproteins that includes both inhibitory and activating receptors (36). Although Ly49 receptors have their signaling domain (CYT-TM) at the amino-terminus, compared with the carboxy-terminus for KIR, their activating and inhibitory motifs are similar. It was therefore intriguing to see how the evolution of activating *Ly49* compared with that of the activating *KIR*.

Phylogenetic analysis of the signaling domains of mouse and rat *Ly49* family members also included sequences from other species, including the single, nonfunctional human *Ly49* gene. With two exceptions, all of the activating *Ly49* genes form a unique monophyletic group that includes no inhibitory *Ly49*. (The two exceptions are the rat *Ly49s3* and the predicted activating *Ly49C* of the horse; Fig. 6 A). Thus, almost all signaling domains of the activating Ly49 receptors of mouse and rat derive from a single ancestral activating sig-

nal domain. Reconstruction of ancestral sequences for the four nodes indicated by arrows in Fig. 6 A supports a model in which this ancestral activating signaling domain was produced by mutation and functional switch of a rodent inhibitory signaling domain. We estimate that this functional switch occurred 18.5–31 MYA (Table II), indicating it was rodent specific, because the earliest divergence within rodents occurred  $\sim 75$  MYA (37, 38). The activating Ly49 could also be specific to Murinae, because they separated from their closest relatives, the Cricetidae and the Gerbillidae,  $\sim 31$  and  $\sim 34$  MYA (38), respectively, a time at the upper range of our estimate for the functional switch (Table II).

An independent and more recent functional switch must be proposed to account for the formation of the activating rat *Ly49s3* receptor. The clustering of the *Ly49s3* signaling domain with four other rat *Ly49* sequences that have activating (charged residue in the TM) and inhibitory (ITIM in CYT) motifs points to this evolution having first involved the acquisition of a charged residue in the transmembrane region followed by loss of ITIM from the cytoplasmic tail. This model is also supported by reconstruction of the ancestral signaling domain shared by *Ly49s3* and its close relatives. That these are all rat sequences raises the possibility of a rat-specific emergence. However, an analysis of the time of emergence of this receptor indicates a range of  $\sim 3.5$  to 15.5 MYA (Table II), leaving open the alternative possibility that receptor emergence preceded the mouse and rat separation,  $\sim 13$ – $21$  MYA (37).

The tight clustering observed for the signaling domains of most rat and mouse activating Ly49 receptors (Fig. 6 A)



panded in the human species to give the diversity of group B *KIR* haplotypes. The STK share a common ancestor that was an inhibitory KIR. Reconstructing such evolution of an activating KIR from an inhibitory KIR shows that it occurred only once in hominoids and involved as few as five to seven nucleotide changes. These changes introduced a charged residue into the transmembrane domain and altered both the length and the sequence of the cytoplasmic tail to eliminate the ITIMs. By this process of functional shift, the first hominoid STK emerged 13.5–18 MYA. Subsequently, additional STK were formed through the action of two other evolutionary mechanisms: recombination, which replaced the signaling domain of inhibitory receptors with the

activating domain, and, to a lesser extent, duplication of *STK* genes with subsequent divergence of the daughter genes (Fig. 7 A). The activating *Ly49* genes evolved by similar processes from inhibitory *Ly49* genes.

The signaling domains of the activating KIR in rhesus monkey and cattle are unrelated to those of the hominoids, indicating that this form of signaling domain has evolved independently in different species at different times. The formation of activating receptors from inhibitory receptors is seen to be a recurrent process. This recurrence is no coincidence, because of the competitive advantage of new variant receptors that can engage an adaptor molecule (e.g., DAP12), which is part of an existing pathway of activating

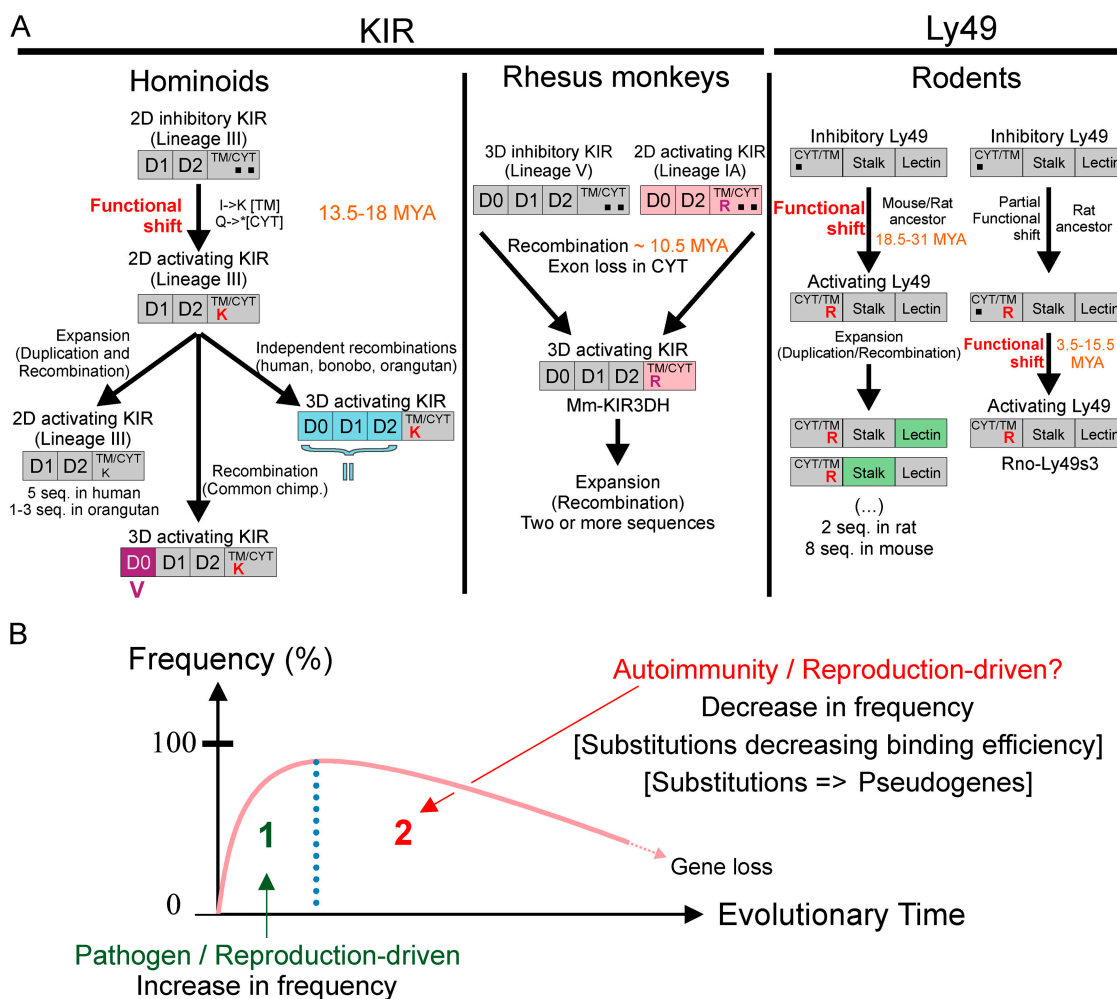


**Figure 7. Model for the emergence and loss of activating KIR and Ly49.** (A) An inferred history for the origin and spread of hominoid STK, rhesus monkey KIR3DH, and activating Ly49 in rodents is shown. Boxes represent the different protein domains. For the signaling domain, charged residues and ITIMs are represented by the corresponding amino acid and by a filled square, respectively. When recombinant structures are present, the lineage of the recombinant domains is indicated by a roman letter below the domain. (B) Two-stage model for the emergence and loss of activating

KIR and Ly49. The creation of an activating receptor is followed by a rapid increase in frequency caused by the beneficial effects (resistance to pathogens, increase in reproductive success). When the selective advantage of the activating receptor disappears, its negative effects (disabilities caused by autoimmunity or a detrimentally high birthrate) lead to decreasing frequency and eventual gene loss. Alternatively, or in parallel to this decrease in frequency, substitutions that decrease or eliminate the function of the activating receptor can occur and be selected.

signal transduction. Such activating receptors therefore will tend to be selected.

Although the signaling adaptors have been conserved for more than 400 million years, and both KIR and Ly49 have existed for at least 100 million years, none of the modern-day activating KIR or Ly49 are older than  $\sim 18$  and  $\sim 31$  million years, respectively. The recurrent creation of activating receptors and the absence of ancient lineages of activating receptors indicates that activating receptors are short lived: they are periodically made, lost, and reinvented, rather than being preserved by strong, persistent selection. Further evidence for this dynamic comes from the distribution of STK in human populations. Overall, the STK have lower frequencies than the inhibitory KIR (41–43), and in some populations (e.g., the Japanese) the frequencies of STK and group B KIR haplotypes are very low (43). None of the STK genes is fixed, and because a common allele of *KIR2DS4*—the single STK of the group A haplotypes—is probably nonfunctional, many millions of healthy people have no STK at all. These observations all point to natural selection having the capacity to select for or against activating KIR and Ly49, depending on circumstance.

The functions of inhibitory KIR are better understood than those of activating KIR. They are MHC class I receptors that help NK cells be tolerant of healthy autologous cells but reactive toward cells having perturbed MHC class I expression (44). In humans, HLA-C is the major inhibitory ligand; all HLA-C allotypes engage inhibitory KIR2DL, and most KIR haplotypes and genotypes encode inhibitory KIR specific for two broad groups of HLA-C ligand, C1 and C2 (45). By contrast, a minority of HLA-A and -B allotypes are inhibitory ligands, and a significant proportion of KIR haplotypes do not encode a functional inhibitory HLA-B receptor.

The interaction of HLA-C1 with its cognate receptors KIR2DL2 and -3 is weaker than that for HLA-C2 and KIR2DL1 (15, 46). Such polymorphism, combined with independent segregation of KIR and HLA-C, means that individuals differ qualitatively and quantitatively in their NK cell regulation by HLA-C. Consequently, individuals having only the weaker inhibition mediated by C1 binding to KIR2DL3 are more likely to resolve acute hepatitis C virus infections (47), presumably because their NK cells are more readily activated. Other correlative studies show that weaker inhibitory KIR–HLA-C interactions and/or the presence of activating STK is associated with slower progression of HIV infections to AIDS (19) and reduced risk of preeclampsia in pregnancy (48). Conversely, group B KIR haplotypes, with their STK, are also associated with an increased likelihood of autoimmune diseases such as psoriasis (49, 50), psoriatic arthritis (20, 51), type I diabetes (22), scleroderma (52), and vascular complications of rheumatoid arthritis (21).

These clinical correlations indicate that the potential advantages of STK are improvement in the response to infection and increased reproductive success; they also indicate that their potential disadvantage is increased disability result-

ing from autoimmunity. Although autoimmunity has often been dismissed as a factor in natural selection, because it usually affects people past reproductive age, such conjecture ignores the important contributions that healthy older relatives, notably grandparents, could have made to raising children. During episodes of epidemic viral infection, genotypes containing STK are more likely to be advantageous and selected, whereas in periods when infections are less pressing, genotypes without STK could gain the competitive advantage. The short life of activating KIR and Ly49 can therefore be explained by a two-stage model: a first stage, in which a low-frequency activating receptor is rapidly driven to high frequency because of its beneficial effect, is followed by a second stage during which the benefit is outweighed by the detriment, leading to decreasing frequency and eventual loss of the activating receptor gene (Fig. 7 B).

Although the clinical correlations point to their influence, the manner by which the STK exert their effects is uncertain, because their ligands have yet to be defined. Although the ligand-binding domains of KIR2DS1 and KIR2DL1 are similar, as are those of KIR2DS2 and KIR2DL2/3, the STK have little, if any, affinity for HLA-C. Indeed, mutational and structural analysis shows that KIR2DS1 and KIR2DS2 have each acquired a single-amino acid substitution that prevents the binding of C2 and C1, respectively (15–18). One possibility is that KIR2DS binding is much more dependent on the peptide bound by HLA-C than is KIR2DL binding, as reported for KIR3DL2 (53). Alternatively, receptors that were originally selected by infection as activating HLA-C receptors, may have subsequently become attenuated or inactivated when the disease was no longer a threat. Support for this alternative is found with the Ly49 family, because several *Ly49* pseudogenes would encode activating receptors in the absence of frameshifts (see Fig. 6 A for example).

The hominoid STK emerged at a time,  $\sim 13.5$ – $18$  MYA, soon after the previously isolated continents of Africa and Eurasia were connected,  $\sim 18$  MYA (54). This event facilitated the migration of many African mammals to Eurasia, including hominoids, for which fossils unearthed in Europe date to as early as 16–17 MYA (55). Several authors have proposed that the hominoids who migrated to Eurasia eventually gave rise to humans and the other surviving hominoid species (55). In that circumstance, the period starting  $\sim 18$  MYA would have been one of environmental upheaval for hominoid ancestors. The resulting stress and pressure on their immune systems might well have contributed to the selection of a new variety of activating KIR. Through recombination and gene duplication, this ancestral STK would eventually lead to the expanded family of STK present in modern hominoids. The expansion also witnessed striking parallels in evolution (e.g., the independent formation of activating KIR with three Ig domains in bonobos, orangutans, and humans). This parallelism emphasizes the importance of natural selection, not only in the emergence of activating KIR, but also in their expansion and diversification.

## MATERIALS AND METHODS

**Datasets and alignments.** Our *KIR* dataset included all known *KIR* loci and sequences having >1% divergence. The signaling domain analyses were performed using the sequences from exon 7–9. Sequences with the longest 3' untranslated regions were chosen. *Cg-KIR2DL6*, *Cg-KIR2DLc*, *Pt-KIR3DL6*, *Pp-KIR3DL4*, and *Pt-KIRC1* were not used for analysis of the signaling domain, because they are recombinants that give divergent phylogenetic signals for the TM and CYT (24). *KIR3DS1* and *KIR3DL1* were also found to have divergent signals within the CYT domain (unpublished data), and part of the 3' untranslated region sequence was removed to avoid bias. *Bta-KIR2DS1* was too short for analysis of the TM and CYT domains. The 3' ends of the nonprimate *KIR* sequences were trimmed to conserve only the well-aligned parts.

To obtain a *DAP12* dataset, BLAST (56) searches were made of National Center for Biotechnology Information's nonredundant and expressed sequence tags databases. This search also revealed *DAP10*, *CD3 $\gamma$ / $\delta$* , and *CD3 $\epsilon$*  sequences, which we included in the analysis. The *FCER1G* dataset was obtained similarly to the *DAP12* dataset but also includes *CD3 $\zeta$*  sequences.

An *Ly49* dataset was assembled following BLAST searches. Full-length rat sequences predicted based on genomic DNA were also included (57). Groups of sequences with <1% divergence were represented by one sequence. Alignment columns containing single sequences were discarded, as were the insertions found in several sequences that did not align (divergent splice variants).

*KIR* and *Ly49* nucleotide sequences were aligned using MAFFT (58) and were corrected manually; *DAP12* and *FCER1G* amino acid alignments were generated using T-coffee (59).

**Phylogenetic analyses.** Before the analysis of each dataset, we checked for composition bias using a  $\chi^2$  test ( $\alpha = 0.05$ ). For nucleotide sequence analyses, we selected the model of DNA substitution using the Akaike information criterion as implemented in Modeltest 3.06 (60). Neighbor-joining (NJ) analyses were performed with MEGA3 (61) using 1,000 replicates, pairwise comparisons, midpoint rooting, and, in all but one case, the Tamura-Nei method. Because of sequence composition bias with three sequences in Fig. 1 A (mouse and rat *KIR3DL1*:  $P < 0.001$ ; horse *KIR3DL001*:  $P < 0.05$ ), we used the LogDet method. To define groups, we performed the interior branch test (62). For Bayesian analyses we used MrBayes3b4 (63) and conducted three independent runs for each dataset (see supplemental Materials and methods, available at <http://www.jem.org/cgi/content/full/jem.20042558/DC1>). The three topologies obtained were compared statistically using the Shimodaira-Hasegawa test of alternative phylogenetic hypotheses, as implemented in PAUP\*4.0b10 (Sinauer), with resampling estimated log-likelihood optimization and 10,000 bootstrap replicates. This comparison was made with the maximum likelihood model defined by Modeltest. For all the analyses presented, the test failed to reject any of the alternative tree topologies ( $\alpha = 0.05$ ). PAUP\*4.0b10 and the tree bisection-reconnection branch swapping algorithm were used for maximum likelihood and parsimony analyses, with 500 replicates and Modeltest parameters for the former and 1,000 replicates and a heuristic search for the latter.

The analyses of amino acid sequences were performed similarly to the analyses of the nucleotide sequences with the following differences: NJ analyses were performed using a Poisson correction; the Bayesian analyses were conducted using a BLOSOM matrix and gamma distances; and the resulting tree topologies were statistically compared using the Templeton test with a parsimony model ( $\alpha = 0.05$ ).

In the analysis of each dataset, the tree topologies obtained with the different methods were compared using the Shimodaira-Hasegawa test or the Templeton test as described previously. In all analyses but one, the test failed to reject any topology. The NJ tree presented in Fig. 6 A was less likely than the other two trees (Shimodaira-Hasegawa test,  $P < 0.05$ ). Because the difference was not significant at a 1% level, and because the nodes responsible affected only terminal branches, which were not discussed in the analysis, the NJ tree was kept.

**Ancestral sequence reconstruction.** Ancestral sequences were reconstructed using the marginal reconstruction approach of PAML (64) and Bayesian analysis using MrBayes2.01. Marginal reconstruction used the model of DNA substitution defined by Modeltest. Bayesian analyses were as described previously, except that nodes for which ancestral sequence reconstruction was sought were constrained. More than five runs were performed, and a consensus was generated.

**Estimation of divergence time.** Mean, standard deviation, and 95% confidence interval values for divergence times were estimated using the Bayesian relaxed molecular clock approach with the Multidistribute program package (reference 65 and see supplemental Material and methods).

For the *KIR* dataset, the two topologies of Fig. 2 were used, the mean of the prior distribution of the root of the ingroup tree was set to  $27 \pm 3$  MYA (hominoid–Old World monkey separation), and two nodes in the lineage II and *STK* groups were constrained between 10 and 18 MYA (separation of orangutans from humans and African apes). For the *Mm-KIR3DH* dataset, the tree topology of model 1 in Fig. 2 was used, and the root of the ingroup tree was set to  $27 \pm 3$  MYA (hominoid–Old World monkey separation). For the *Ly49* dataset, a modified version of the tree topology obtained in the Bayesian analysis performed for Fig. 6 A was used; the root of the ingroup tree was set to  $87.5 \pm 3.5$  MYA (primate–rodent separation), and three internal calibrations corresponding to the divergence between mouse and rat (13–21 MYA) were used (see online supplemental Material and methods).

**Analysis of functional constraints.** Sequences containing insertions or deletions that changed the reading frame size were removed, as were sequences having premature stop codons. The final stop codons were removed, as were the positions with gaps. The number of  $d_S$  and  $d_N$  were estimated using MEGA3 with the modified Nei-Gojobori method (p-distance). The transition/transversion ratio was estimated using TreePuzzle (66). The SEs were estimated by the bootstrap method (10,000 replicates). The statistical significance of the  $d_N/d_S$  ratios comparing to the neutrality hypothesis was assessed through a two-tailed Z-test.

**Online supplemental material.** Detailed methods for the Bayesian phylogenetic analyses, the divergence time analyses, the analysis presented in Fig. 3 A, and the accession numbers for the sequences used are described in supplemental Material and methods. Online supplemental material is available at <http://www.jem.org/cgi/content/full/jem.20042558/DC1>.

This study was supported by National Institutes of Health grant no. 5 R01 AI24258 (to P. Parham).

The authors have no conflicting financial interests.

Submitted: 16 December 2004

Accepted: 10 March 2005

## REFERENCES

- Biron, C.A., K.B. Nguyen, G.C. Pien, L.P. Cousens, and T.P. Salazar-Mather. 1999. Natural killer cells in antiviral defense: function and regulation by innate cytokines. *Annu. Rev. Immunol.* 17:189–220.
- French, A.R., and W.M. Yokoyama. 2003. Natural killer cells and viral infections. *Curr. Opin. Immunol.* 15:45–51.
- Diefenbach, A., and D.H. Raulet. 2002. The innate immune response to tumors and its role in the induction of T-cell immunity. *Immunol. Rev.* 188:9–21.
- Dupont, B., and K.C. Hsu. 2004. Inhibitory killer Ig-like receptor genes and human leukocyte antigen class I ligands in hematopoietic stem cell transplantation. *Curr. Opin. Immunol.* 16:634–643.
- Moffett-King, A. 2002. Natural killer cells and pregnancy. *Nat. Rev. Immunol.* 2:656–663.
- Lanier, L.L. 2003. Natural killer cell receptor signaling. *Curr. Opin. Immunol.* 15:308–314.
- McQueen, K.L., and P. Parham. 2002. Variable receptors controlling activation and inhibition of NK cells. *Curr. Opin. Immunol.* 14:615–621.

8. Moretta, L., and A. Moretta. 2004. Killer immunoglobulin-like receptors. *Curr. Opin. Immunol.* 16:626–633.
9. Barten, R., M. Torkar, A. Haude, J. Trowsdale, and M.J. Wilson. 2001. Divergent and convergent evolution of NK-cell receptors. *Trends Immunol.* 22:52–57.
10. Uhrberg, M., N.M. Valiante, B.P. Shum, H.G. Shilling, K. Lienert-Weidenbach, B. Corliss, D. Tyan, L.L. Lanier, and P. Parham. 1997. Human diversity in killer cell inhibitory receptor genes. *Immunity.* 7:753–763.
11. Hsu, K.C., X.R. Liu, A. Selvakumar, E. Mickelson, R.J. O'Reilly, and B. Dupont. 2002. Killer Ig-like receptor haplotype analysis by gene content: evidence for genomic diversity with a minimum of six basic framework haplotypes, each with multiple subsets. *J. Immunol.* 169: 5118–5129.
12. Maxwell, L.D., A. Wallace, D. Middleton, and M.D. Curran. 2002. A common KIR2DS4 deletion variant in the human that predicts a soluble KIR molecule analogous to the KIR1D molecule observed in the rhesus monkey. *Tissue Antigens.* 60:254–258.
13. Yawata, M., N. Yawata, L. Abi-Rached, and P. Parham. 2002. Variation within the human killer cell immunoglobulin-like receptor (KIR) gene family. *Crit. Rev. Immunol.* 22:463–482.
14. Arase, H., and L.L. Lanier. 2004. Specific recognition of virus-infected cells by paired NK receptors. *Rev. Med. Virol.* 14:83–93.
15. Winter, C.C., J.E. Gumperz, P. Parham, E.O. Long, and N. Wagtmann. 1998. Direct binding and functional transfer of NK cell inhibitory receptors reveal novel patterns of HLA-C allotype recognition. *J. Immunol.* 161:571–577.
16. Biassoni, R., A. Pessino, A. Malaspina, C. Cantoni, C. Bottino, S. Sivori, L. Moretta, and A. Moretta. 1997. Role of amino acid position 70 in the binding affinity of p50.1 and p58.1 receptors for HLA-Cw4 molecules. *Eur. J. Immunol.* 27:3095–3099.
17. Vales-Gomez, M., H.T. Reyburn, R.A. Erskine, and J. Strominger. 1998. Differential binding to HLA-C of p50-activating and p58-inhibitory natural killer cell receptors. *Proc. Natl. Acad. Sci. USA.* 95:14326–14331.
18. Saulquin, X., L.N. Gastinel, and E. Vivier. 2003. Crystal structure of the human natural killer cell activating receptor KIR2DS2 (CD158j). *J. Exp. Med.* 197:933–938.
19. Martin, M.P., X. Gao, J.H. Lee, G.W. Nelson, R. Detels, J.J. Goedert, S. Buchbinder, K. Hoots, D. Vlahov, J. Trowsdale, et al. 2002. Epistatic interaction between KIR3DS1 and HLA-B delays the progression to AIDS. *Nat. Genet.* 31:429–434.
20. Martin, M.P., G. Nelson, J.H. Lee, F. Pellett, X. Gao, J. Wade, M.J. Wilson, J. Trowsdale, D. Gladman, and M. Carrington. 2002. Cutting edge: susceptibility to psoriatic arthritis: influence of activating killer Ig-like receptor genes in the absence of specific HLA-C alleles. *J. Immunol.* 169:2818–2822.
21. Yen, J.H., B.E. Moore, T. Nakajima, D. Scholl, D.J. Schaid, C.M. Weyand, and J.J. Goronzy. 2001. Major histocompatibility complex class I-recognizing receptors are disease risk genes in rheumatoid arthritis. *J. Exp. Med.* 193:1159–1167.
22. van der Slik, A.R., B.P. Koelman, W. Verduijn, G.J. Bruining, B.O. Roep, and M.J. Giphart. 2003. KIR in type 1 diabetes: disparate distribution of activating and inhibitory natural killer cell receptors in patients versus HLA-matched control subjects. *Diabetes.* 52:2639–2642.
23. Lee, S.H., S. Girard, D. Macina, M. Busa, A. Zafer, A. Belouchi, P. Gros, and S.M. Vidal. 2001. Susceptibility to mouse cytomegalovirus is associated with deletion of an activating natural killer cell receptor of the C-type lectin superfamily. *Nat. Genet.* 28:42–45.
24. Rajalingam, R., P. Parham, and L. Abi-Rached. 2004. Domain shuffling has been the main mechanism forming new hominoid killer cell Ig-like receptors. *J. Immunol.* 172:356–369.
25. Vivier, E., J.A. Nunes, and F. Vely. 2004. Natural killer cell signaling pathways. *Science.* 306:1517–1519.
26. Lanier, L.L., B.C. Corliss, J. Wu, C. Leong, and J.H. Phillips. 1998. Immunoreceptor DAP12 bearing a tyrosine-based activation motif is involved in activating NK cells. *Nature.* 391:703–707.
27. Page, S.L., and M. Goodman. 2001. Catarrhine phylogeny: noncoding DNA evidence for a diphyletic origin of the mangabeys and for a human-chimpanzee clade. *Mol. Phylogenet. Evol.* 18:14–25.
28. Pilbeam, D., and N. Young. 2004. Hominoid evolution: synthesizing disparate data. *C.R. Palevol.* 3:303–319.
29. Faure, M., and E.O. Long. 2002. KIR2DL4 (CD158d), an NK cell-activating receptor with inhibitory potential. *J. Immunol.* 168:6208–6214.
30. Kikuchi-Maki, A., S. Yusa, T.L. Catina, and K.S. Campbell. 2003. KIR2DL4 is an IL-2-regulated NK cell receptor that exhibits limited expression in humans but triggers strong IFN- $\gamma$  production. *J. Immunol.* 171:3415–3425.
31. Goodridge, J.P., C.S. Witt, F.T. Christiansen, and H.S. Warren. 2003. KIR2DL4 (CD158d) genotype influences expression and function in NK cells. *J. Immunol.* 171:1768–1774.
32. LaBonte, M.L., K.L. Hershberger, B. Korber, and N.L. Letvin. 2001. The KIR and CD94/NG2 families of molecules in the rhesus monkey. *Immunol. Rev.* 183:25–40.
33. Grendell, R.L., A.L. Hughes, and T.G. Golos. 2001. Cloning of rhesus monkey killer-cell Ig-like receptors (KIRs) from early pregnancy decidua. *Tissue Antigens.* 58:329–334.
34. Kikuchi-Maki, A., T.L. Catina, and K.S. Campbell. 2005. Cutting edge: KIR2DL4 transduces signals into human NK cells through association with Fc receptor  $\gamma$  protein. *J. Immunol.* 174:3859–3863.
35. Welch, A.Y., M. Kasahara, and L.M. Spain. 2003. Identification of the mouse killer immunoglobulin-like receptor-like (Kirl) gene family mapping to chromosome X. *Immunogenetics.* 54:782–790.
36. Anderson, S.K., J.R. Ortaldo, and D.W. McVicar. 2001. The ever-expanding Ly49 gene family: repertoire and signaling. *Immunol. Rev.* 181:79–89.
37. Springer, M.S., W.J. Murphy, E. Eizirik, and S.J. O'Brien. 2003. Placental mammal diversification and the Cretaceous-Tertiary boundary. *Proc. Natl. Acad. Sci. USA.* 100:1056–1061.
38. Adkins, R.M., E.L. Gelke, D. Rowe, and R.L. Honeycutt. 2001. Molecular phylogeny and divergence time estimates for major rodent groups: evidence from multiple genes. *Mol. Biol. Evol.* 18:777–791.
39. Kasahara, M., T. Suzuki, and L.D. Pasquier. 2004. On the origins of the adaptive immune system: novel insights from invertebrates and cold-blooded vertebrates. *Trends Immunol.* 25:105–111.
40. Vilches, C., and P. Parham. 2002. KIR: diverse, rapidly evolving receptors of innate and adaptive immunity. *Annu. Rev. Immunol.* 20:217–251.
41. Norman, P.J., H.A. Stephens, D.H. Verity, D. Chandanayingyong, and R.W. Vaughan. 2001. Distribution of natural killer cell immunoglobulin-like receptor sequences in three ethnic groups. *Immunogenetics.* 52:195–205.
42. Norman, P.J., C.V. Carrington, M. Byng, L.D. Maxwell, M.D. Curran, H.A. Stephens, D. Chandanayingyong, D.H. Verity, K. Hameed, D.D. Ramdath, et al. 2002. Natural killer cell immunoglobulin-like receptor (KIR) locus profiles in African and South Asian populations. *Genes Immun.* 3:86–95.
43. Yawata, M., N. Yawata, K.L. McQueen, N.W. Cheng, L.A. Guethlein, R. Rajalingam, H.G. Shilling, and P. Parham. 2002. Predominance of group A KIR haplotypes in Japanese associated with diverse NK cell repertoires of KIR expression. *Immunogenetics.* 54:543–550.
44. Ljunggren, H.G., and K. Karre. 1990. In search of the 'missing self': MHC molecules and NK cell recognition. *Immunol. Today.* 11:237–244.
45. Colonna, M., G. Borsellino, M. Falco, G.B. Ferrara, and J.L. Strominger. 1993. HLA-C is the inhibitory ligand that determines dominant resistance to lysis by NK1- and NK2-specific natural killer cells. *Proc. Natl. Acad. Sci. USA.* 90:12000–12004.
46. Boyington, J.C., and P.D. Sun. 2002. A structural perspective on MHC class I recognition by killer cell immunoglobulin-like receptors. *Mol. Immunol.* 38:1007–1021.
47. Khakoo, S.I., C.L. Thio, M.P. Martin, C.R. Brooks, X. Gao, J. Astemborski, J. Cheng, J.J. Goedert, D. Vlahov, M. Hilgartner, et al. 2004. HLA and NK cell inhibitory receptor genes in resolving hepatitis C virus infection. *Science.* 305:872–874.
48. Hiby, S.E., J.J. Walker, M. O'Shaughnessy K, C.W. Redman, M. Carrington, J. Trowsdale, and A. Moffett. 2004. Combinations of maternal KIR and fetal HLA-C genes influence the risk of preeclampsia and reproductive success. *J. Exp. Med.* 200:957–965.

49. Luszczek, W., M. Manczak, M. Cislo, P. Nockowski, A. Wisniewski, M. Jasek, and P. Kusnierczyk. 2004. Gene for the activating natural killer cell receptor, KIR2DS1, is associated with susceptibility to psoriasis vulgaris. *Hum. Immunol.* 65:758–766.
50. Suzuki, Y., Y. Hamamoto, Y. Ogasawara, K. Ishikawa, Y. Yoshikawa, T. Sasazuki, and M. Muto. 2004. Genetic polymorphisms of killer cell immunoglobulin-like receptors are associated with susceptibility to psoriasis vulgaris. *J. Invest. Dermatol.* 122:1133–1136.
51. Nelson, G.W., M.P. Martin, D. Gladman, J. Wade, J. Trowsdale, and M. Carrington. 2004. Cutting edge: heterozygote advantage in autoimmune disease: hierarchy of protection/susceptibility conferred by HLA and killer Ig-like receptor combinations in psoriatic arthritis. *J. Immunol.* 173:4273–4276.
52. Momot, T., S. Koch, N. Hunzelmann, T. Krieg, K. Ulbricht, R.E. Schmidt, and T. Witte. 2004. Association of killer cell immunoglobulin-like receptors with scleroderma. *Arthritis Rheum.* 50:1561–1565.
53. Hansasuta, P., T. Dong, H. Thananchai, M. Weekes, C. Willberg, H. Aldemir, S. Rowland-Jones, and V.M. Braud. 2004. Recognition of HLA-A3 and HLA-A11 by KIR3DL2 is peptide-specific. *Eur. J. Immunol.* 34:1673–1679.
54. Waddell, P.J., and D. Penny. 1996. Evolutionary trees of apes and humans from DNA sequences. In *Handbook of Human Symbolic Evolution*. A. Lock and C.R. Peters, editors. Oxford University Press, Oxford. 53–73.
55. Begun, D.R., E. Güleç, and D. Geraads. 2003. Dispersal patterns of Eurasian hominoids: implications from Turkey. *Deinsea.* 10:23–39.
56. Altschul, S.F., T.L. Madden, A.A. Schaffer, J. Zhang, Z. Zhang, W. Miller, and D.J. Lipman. 1997. Gapped BLAST and PSI-BLAST: a new generation of protein database search programs. *Nucleic Acids Res.* 25:3389–3402.
57. Wilhelm, B.T., and D.L. Mager. 2004. Rapid expansion of the Ly49 gene cluster in rat. *Genomics.* 84:218–221.
58. Katoh, K., K. Misawa, K. Kuma, and T. Miyata. 2002. MAFFT: a novel method for rapid multiple sequence alignment based on fast Fourier transform. *Nucleic Acids Res.* 30:3059–3066.
59. Notredame, C., D.G. Higgins, and J. Heringa. 2000. T-Coffee: a novel method for fast and accurate multiple sequence alignment. *J. Mol. Biol.* 302:205–217.
60. Posada, D., and K.A. Crandall. 1998. MODELTEST: testing the model of DNA substitution. *Bioinformatics.* 14:817–818.
61. Kumar, S., K. Tamura, and M. Nei. 2004. MEGA3: integrated software for molecular evolutionary genetics analysis and sequence alignment. *Brief. Bioinformatics.* 5:150–163.
62. Sitnikova, T. 1996. Bootstrap method of interior-branch test for phylogenetic trees. *Mol. Biol. Evol.* 13:605–611.
63. Ronquist, F., and J.P. Huelsenbeck. 2003. MrBayes 3: Bayesian phylogenetic inference under mixed models. *Bioinformatics.* 19:1572–1574.
64. Yang, Z. 1997. PAML: a program package for phylogenetic analysis by maximum likelihood. *Comput. Appl. Biosci.* 13:555–556.
65. Thorne, J.L., and H. Kishino. 2002. Divergence time and evolutionary rate estimation with multilocus data. *Syst. Biol.* 51:689–702.
66. Schmidt, H.A., K. Strimmer, M. Vingron, and A. von Haeseler. 2002. TREE-PUZZLE: maximum likelihood phylogenetic analysis using quartets and parallel computing. *Bioinformatics.* 18:502–504.
67. Takahashi, T., M. Yawata, T. Raudsepp, T.L. Lear, B.P. Chowdhary, D.F. Antczak, and M. Kasahara. 2004. Natural killer cell receptors in the horse: evidence for the existence of multiple transcribed LY49 genes. *Eur. J. Immunol.* 34:773–784.